Comparative Reactivity of Triruthenium and Triosmium μ_3-η^2-Imidoyls. 1. Dynamics and Reactions with Carbon Monoxide, Phosphine, and Isocyanide

Edward Rosenberg*

Department of Chemistry, The University of Montana, Missoula, Montana 59812

Luciano Milone,* Roberto Gobetto, and Domenico Osella

Dipartimento di Chimica IFM, Università di Torino, via P. Giuria 7-9, 10125 Torino, Italy

Kenneth Hardcastle,* Sharad Hajela, Kate Moizeau, Michael Day, Erich Wolf, and David Espitia

Department of Chemistry, California State University, Northridge, California 91330

Received December 23, 1996[⊗]

The reactivity and ligand dynamics of the μ_3-η^2-imidoyl clusters $Ru_3(CO)_9(\mu_3$-η^2-RC═NR′)-(μ-H) (R = CH_3, R′ = Et **2**; RR′ = $(CH_2)_3$, **3**; RR′ = $(CH_2)_2C(H)CH_2OCH_3$ **4**, R = R′ = CH_3, **5**) are compared with the previously reported osmium analogs. The lowest energy dynamical process in these clusters is the "windshield wiper" motion over the face of the cluster whereas tripodal rotation of the carbonyl groups on the unbridged metal atom is the fastest process in the analogous osmium compounds. Although the structures of the phosphine and isocyanide substitution products reported, $Ru_3(CO)_8(\mu_3$-η^2-RC═NR′)(μ-H)L (R = CH_3, R′ = CH_2CH_3, L = PPh_3 (**8a**), L = CNMe (**12**); R = R′ = $(CH_2)_3$, L = PPh_3 (**9**), L = CNMe (**13**); R = R′ = CH_3, L = PPh_3 (**10**), are identical to their osmium analogs, the pathway to their formation reflects the lower CO dissociation energies for ruthenium clusters and a greater sensitivity to the substituents on the imidoyl group. The solid state structures of **9** and **12** are reported as well as that of $Os_3(CO)_8(\mu$-η^2-C═N$(CH_2)_3(\mu$-H)(PPh_3)(MeNC) (**15**). The latter illustrates the hemilabile nature of the μ_3-imidoyl ligand even in phosphine-substituted derivatives and the structural preferences of phosphine and isocyanide ligands in this class of clusters.

Introduction

In recent years, several research groups have synthesized a range of μ_3-η^2-imidoyl clusters of the type $M_3(\mu_3$-η^2-RC═NR′)(μ-H)$(L)_n$ (M = Co, Fe, Ru, Rh, Os; L = η^5-C_5H_5, n = 3; L = CO, n = 9).[1] These clusters all exhibit a common dynamical process, the so-called "windshield wiper" motion usually pivoting on the carbon atom (Scheme 1). The activation energies for this process, in the range 40−55 kJ/mol, are in the order Os > Ru > Fe ≈ Co.[1] More interestingly, although these clusters are all 48e⁻, valence-saturated clusters, they are susceptible to ligand addition reactions (Scheme 2, structure A)[1g,i] at ambient temperature. Their overall reactivity closely parallels electron deficient 46e⁻ trimetallic species, rather than their 48e⁻ μ_3-η^2-hydrocarbyl analogs. It was originally thought that the facile motion of ligands in these μ_3-η^2-imidoyl clusters was directly related to the exceptional reactivity of this class of compounds.[1g,h] However, a recent kinetic investigation of phosphine addition to the stereochemically rigid $Os_3(CO)_8(\mu_3$-η^2-C═N$(CH_2)_3(\mu_3$-H)$_2$H suggests that ligand addition rate relates only to the facile displacement of the carbon−nitrogen double bond relative to related multiple bonds in μ_3-η^2-hydrocarbyl ligands.[2] Related stereochemical studies have shown that displacement of the carbon−nitrogen double bond occurs by a dis-

Scheme 1. "Windshield Wiper Motion" in μ_3-Imidoyls (Shown Here L_n = $(CO)_9$, M = Ru, Os)

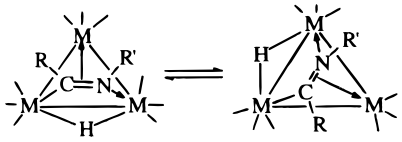

[⊗] Abstract published in *Advance ACS Abstracts,* May 15, 1997.

(1) (a) Gobetto, R.; Hardcastle, K. I.; Kabir, S. E.; Milone, L.; Nishimura, N.; Botta, M.; Rosenberg, E.; Yin, M. *Organometallics* **1995**, *14*, 3068 and references therein. (b) Hansert, B.; Tasi, M.; Tiripicchio, A.; Tiripicchio Camellini, M.; Vahrenkamp, H. *Organometallics* **1991**, *10*, 4070. (c) Süss-Fink, G.; Jenke, T.; Heitz, H.; Pellinghelli, M. A.; Tiripicchio, A. *J. Organomet. Chem.* **1989**, *379*, 311. (d) Basu, A.; Bhaduri, S.; Sharma, K.; Jones, P. G. *J. Chem. Soc., Chem. Commun.* **1987**, 1126. (e) Pellinghelli, M. A.; Tiripicchio, A.; Cabeza, J. A.; Oro, L. A. *J. Chem. Soc., Dalton Trans.* **1990**, 1509. (f) Day, M. W.; Hajela, S.; Kabir, S. E.; Irving, M.; McPhillips, T.; Wolf, E.; Hardcastle, K. I.; Rosenberg, E.; Milone, L.; Gobetto, R.; Osella, D. *Organometallics* **1991**, *10*, 2743 and references therein. (g) Rosenberg, E.; Kabir, S. E.; Day, M.; Hardcastle, K. I.; Irving, M. *J. Cluster Sci.* **1994**, *5*, 481. (h) Day, M.; Espitia, D.; Hardcastle, K. I.; Kabir, S. E.; Rosenberg, E.; Gobetto, R.; Milone, L.; Osella, D. *Organometallics* **1991**, *10*, 3550. (i) Bruce, M. I.; Wallis, R. C. *Aust. J. Chem.* **1982**, *35*, 709. (j) Bhaduri, S.; Sapra, N.; Sharma, K.; Jones, P. G.; Carpenter, J. *J. Chem. Soc., Dalton Trans.* **1990**, 1305. (k) Eisenstadt, A.; Giandomenico, M.; Frederick, M. F.; Laine, R. M. *Organometallics* **1985**, *4*, 2033. (l) Fish, R. H.; Kim, T. J.; Stewart, J. L.; Bushweller, J. H.; Rosen, R. K.; Dupon, J. W. *Organometallics* **1986**, *5*, 2193. (m) Casey, C. P.; Widenhoefer, R. A.; Hallenbeck, S. L.; Hayashi, R. K.; Gavney, J. A. *Organometallics* **1996**, *13*, 4720. (n) McKenna, S. T.; Andersen, R. A.; Muetterties, E. L. *Organometallics* **1986**, *5*, 2233.

(2) Rosenberg, E.; Kabir, S. E.; Day, M.; Hardcastle, K. I. *Organometallics* **1994**, *13*, 4437.

S0276-7333(96)01090-4 CCC: $14.00

Scheme 2. Ligand Addition, Rearrangement, CO Dissociation in Imidoyls (M = Ru, Os)

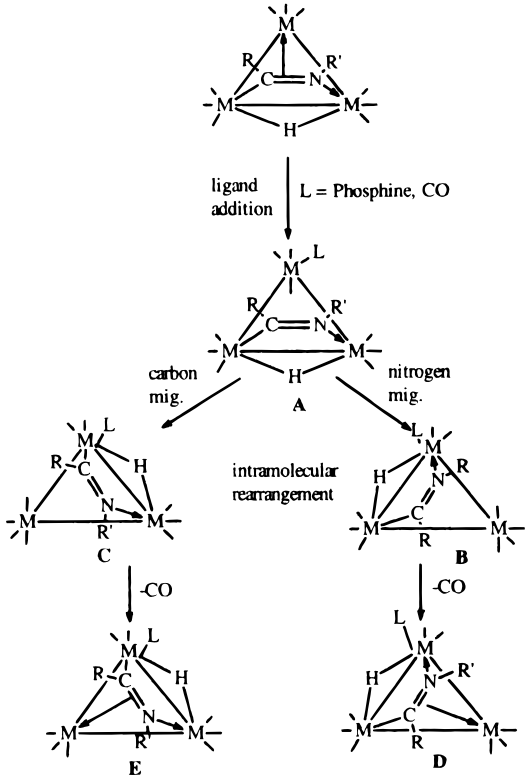

tinctly topside approach of the incoming ligand and that the rate of addition and the binding constant of the ligand are very sensitive to its steric and electronic properties.[3] The initial ligand addition can be followed by carbonyl loss and recoordination of the carbon−nitrogen double bond at ambient or elevated temperatures (Scheme 2, structures D and E).[1g,i] This overall pattern of reactivity places the μ_3-η^2-imidoyl in the category of a "hemilabile" ligand with the potential for undergoing multiple ligand addition−displacement cycles and points to their future development as homogeneous catalysts. In the case of the triosmium clusters, $Os_3(CO)_9(\mu_3\text{-}\eta^2\text{-}C{=}N(CH_2)_3)(\mu\text{-}H)$ (**1**), the stepwise mechanism for the overall μ_3-imidoyl displacement−recoordination process has been elucidated and involves an intermediate intramolecular rearrangement (at 80−90 °C, Scheme 2, structure B) which follows the initial ligand addition (at 25 °C) and precedes carbonyl dissociation and recoordination of the carbon−nitrogen double bond (at 125 °C, Scheme 2, structures D and E).[1g,h]

Thus, the μ_3- to μ- to μ_3-imidoyl cycle appears to take place in three steps: (a) ligand addition, (b) intramolecular rearrangement, and (c) decarbonylation (Scheme 2). The first step is much faster for Ru than for Os, taking place instantaneously at −40 to +25 °C rather than requiring overnight conversions.[3] The ligand addition products, **A**, are kinetically stable at 25 °C for Os, while they are not observed at all for Ru.[3] The rearrangement of **A** to **B** has been shown to involve, for Os with L = phosphine, an intramolecular CO and nitrogen migration.[2] This rearrangement step for osmium appears to pivot on carbon, and carbon migration (structure **C**, Scheme 2), if it occurs at all, is competitive with decarbonylation. In this report, we present evidence that this rearrangement is more rapid for Ru, being as fast as ligand addition and having both carbon and nitrogen migration as accessible processes.

(3) (a) Rosenberg, E.; Freeman, W.; Carlos, Z.; Hardcastle, K. I.; Yoo, Y. J.; Milone, L.; Gobetto, R. *J. Cluster Sci.* **1992**, *3*, 439. (b) Hardcastle, K. I.; Irving, M. *J. Cluster Sci.* **1993**, *4*, 77.

Results and Discussion

A. Reactions of Triruthenium μ_3-η^2-Imidoyls with Carbon Monoxide. We have previously reported the synthesis of the compounds $Ru_3(CO)_9(\mu_3\text{-}\eta^2\text{-}CH_3C{=}NCH_2CH_3)(\mu\text{-}H)$ (**2**) and $Ru_3(CO)_9(\mu_3\text{-}\eta^2\text{-}C{=}N(CH_2)_3)(\mu\text{-}H)$ (**3**), while Süss-Fink and co-workers have reported the related $Ru_3(CO)_9(\mu_3\text{-}\eta^2\text{-}C{=}N(CH(CH_2OCH_3)(CH_2)_2)(\mu\text{-}H)$ (**4**).[1c] In our previous studies of μ_3-imidoyl reactivity, we noted that the groups attached to the imidoyl ligand had a significant impact on the structure of the ligand addition products.[1h,3] We therefore decided to attempt to synthesize $Ru_3(CO)_9(\mu_3\text{-}\eta^2\text{-}CH_3C{=}NCH_3)(\mu\text{-}H)$ (**5**) by the reaction of $N(CH_2CH_3)_2CH_3$ with $Ru_3(CO)_{12}$ using trimethylamine *N*-oxide as a reaction promoter.[1f] Compound **5** was obtained in moderate yield along with significant amounts of **2** and $Ru_3(CO)_{10}(\mu\text{-}\eta^2\text{-}CH_3C{=}NCH_3)(\mu\text{-}H)$ (**6**) (eq 1). The isolation of the decacarbonyl, **6**, as a coproduct is in sharp contrast to the synthesis of **2**−**4**, where only the nonacarbonyls are formed under essentially identical reaction conditions.[1f] This suggests a relationship between the rate of carbonyl dissociation/association and the steric bulk of the imidoyl ligand. We previously noted a similar relationship in triosmium μ_3-η^2-alkyne complexes.[3]

$$Ru_3(CO)_{12} + (CH_3CH_2)_2NCH_3 \xrightarrow[80^\circ C]{(CH_3)_3NO} \quad (1)$$

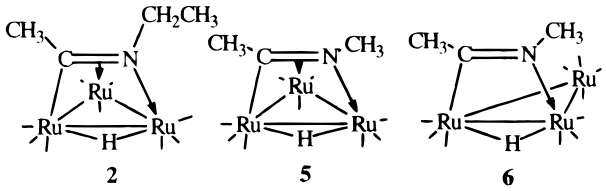

The reaction of **2**−**5** with carbon monoxide takes place rapidly at 1 atm and 25 °C. This process is readily monitored by ^{1}H-NMR where disappearance of hydride signals at −18.00 ppm, associated with **2**−**5**, is coincident with appearance of the hydride resonances associated with their decacarbonyl analogs at about −14 to −15 ppm. This is in sharp contrast to the reaction of the osmium complex, **1**, with carbon monoxide where no significant incorporation is realized below 60 °C.[1h] Conversion of **2**−**5** to their decarbonyl analogs is complete on warming to ambient temperatures when these complexes are exposed to 1 atm of CO at 77 K. No significant selective incorporation of carbon monoxide could be detected in any case.[3] In the particular case of **4**, two isomeric decarbonyl species, **7a** and **7b**, are formed in a ratio of 3:1 (eq 2). This ratio remains unchanged, on standing in solution, as evidenced by ^{1}H-NMR, which shows two hydride resonances at −14.70 and −14.91 ppm and two sets of partially resolved ligand resonances. These results indicate that, with carbon monoxide, the products **7a** and **7b** are formed

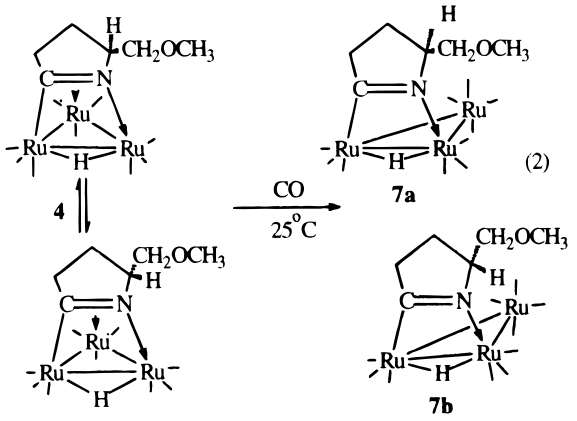

in their thermodynamic ratios. Certainly we cannot exclude a rapid equilibration by carbonyl association/dissociation following initial formation of the decarbonyl. However, at room temperature, incorporation of ^{13}CO into the mixture of **7a** and **7b** proved to be slow with no significant enrichment being observed up to 4 h after exposure to an atmosphere of 90% enriched ^{13}CO. The ratio of the two stereoisomers of **4** is about 1:1.[3a]

These results, taken together with the nonselective carbon monoxide incorporation into **2**−**5**, suggest that the coordination of the incoming ligand, at least in the case of CO, can take place at all three ruthenium atoms. This in turn implies approach of the incoming ligand at the carbon−nitrogen double bond and the coordinated nitrogen (or rapid nitrogen and carbonyl interchange) and also migration of carbon (Scheme 2). Incorporation of ^{13}CO into **1** on the other hand takes place with high selectivity at 60 °C with significant incorporation at only one osmium atom (i.e., the one formerly π-bound to the carbon−nitrogen double bond).[3] In order to further elucidate the origin of these differences, we decided to take a more detailed look at the dynamics of the μ_3-η^2-ruthenium imidoyls.

The VT ^{13}C-NMR of **5** is shown in Figure 1 along with the definitive assignments based on proton-coupled 1D-^{13}C data and the known mode of fluxionality for this type of compound.[4] The 2D-EXSY spectrum of **5** at −90 °C is shown in Figure 2. The lowest energy exchange process for **5** is the windshield wiper process as evidenced by the two intense cross peaks between carbonyls a and b (Figures 1 and 2). The onset of axial−radial exchange at the nitrogen bound ruthenium atom is the second fastest process as evidenced by the observed cross peak between two of the three carbonyls, d and f, on this ruthenium atom. In the case of the osmium complex, **1**, the lowest energy exchange process is the tripodal motion on the osmium atom π-bound to the imidoyl ligand followed by the onset of the windshield wiper motion and then tripodal motion at the nitrogen bound osmium atom.[5] That motion of the carbon atom is an accessible process in complexes such as **2**−**5** is illustrated by the averaging of all carbonyl groups in the high-temperature VT ^{13}C-NMR of **2** (Figure 3). This is a reversible process, and the observed average shift of the broadened peak at 194.30 ppm is in good agreement with the calculated weighted average of the room temperature spectrum (194.34). This averaging process has not been observed for the osmium analogs.[1g,5]

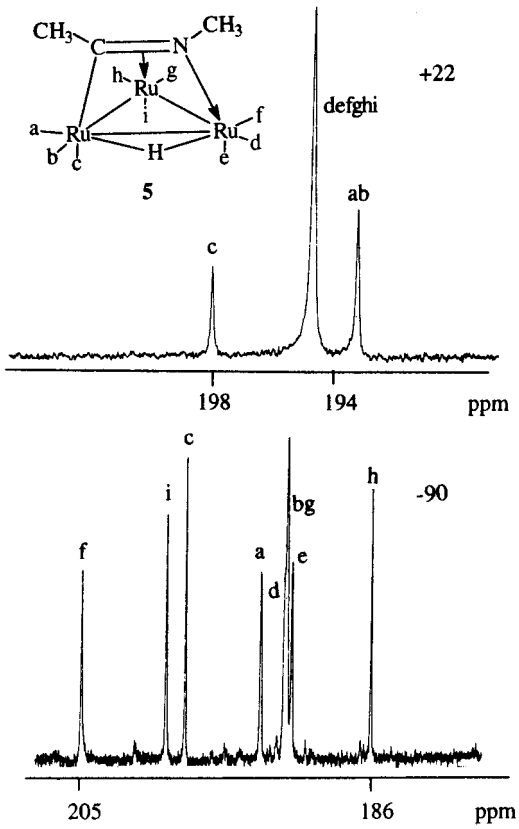

Figure 1. VT ^{13}C-NMR **5** at (a) 22 °C and (b) −90 °C in CD_2Cl_2 at 100 MHz. (Note: the scale for the 22 °C spectrum is different than the −90 °C spectrum.)

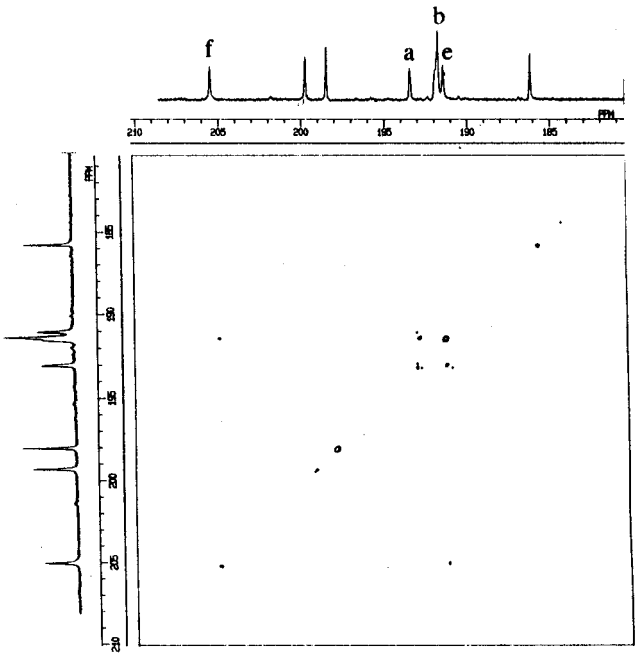

Figure 2. 2D-^{13}C-EXY spectrum of **5** at −90 °C in CD_2Cl_2 at 100 MHz.

B. Reactions of Phosphines with Triruthenium μ_3-Imidoyl Complexes. We previously reported the solid state structure of the product resulting from the addition of triphenylphosphine to **2**, $Ru_3(CO)_8(\mu_3$-η^2-

(4) Aime, S.; Gobetto, R.; Padovan, F.; Botta, M.; Rosenberg, E.; Gellert, R. W. *Organometallics* **1987**, *6*, 2074.
(5) Day, M.; Espitia, D.; Hardcastle, K. I.; Kabir, S. E.; McPhillips, T.; Rosenberg, E.; Gobetto, R.; Milone, L.; Osella, D. *Organometallics* **1993**, *12*, 2309.

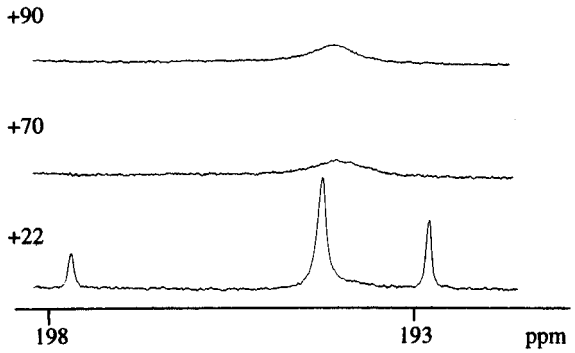

Figure 3. VT ^{13}C-NMR of **2** in toluene-d_8 at 100 MHz.

$CH_3C{=}NCH_2CH_3)(\mu\text{-}H)P(C_6H_5)_3$ (**8a**).[3b] In solution, this product exists in two inseparable isomers **8a** and **8b** in a 2:1 ratio (eq 3). These products are the result of a

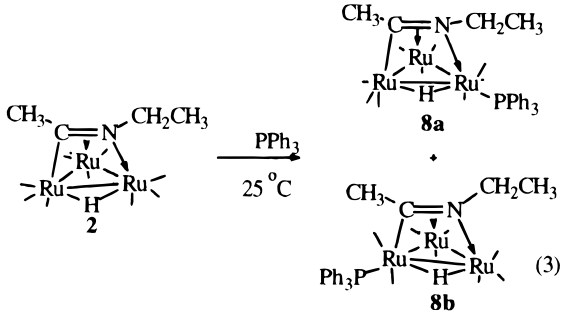

ligand addition−CO dissociation, but the details of the formation of this apparently multistep process and its relationship to Scheme 2 are not clear. The structure of **8b** is based on ^{1}H NMR data. The methyl resonance at 2.01 ppm associated with **8b** shows a phosphorous−hydrogen coupling ($^4J(^{31}P^1H)$ = 2.9 Hz) while the corresponding methyl resonance for **8a** appears as a singlet. As for **8a**, the methylene resonances for **8b** appear as two widely separated AB multiplets at 3.99 and 3.09 ppm (3.00 and 2.51 ppm for **8a**). The similarity in the chemical shifts and phosphorous−hydrogen couplings observed for the hydrides in **8a** and **8b** (−17.2 ppm, $^2J(^{31}P^1H)$ = 15.2 Hz for **8a**; −17.47 ppm, $^2J(^{31}P^1H)$ = 15.3 Hz for **8b**) suggest that the relationship between the hydride and the phosphine is the same in the two isomers. Interestingly, although the hydride resonance of **8b** is sharp at 25 °C, the hydride resonance of **8a** appears somewhat broadened at this temperature but sharpens with decreasing temperature until −60 °C. We attribute this broadening to the averaging of **8a** with an undetectable amount of one or two of the other conformers of **8a** (with the phosphine in the other radial or in an axial position) by axial−radial exchange. That the ligands on the ruthenium atom bound to nitrogen are more fluxional than those on the ruthenium atom bound to the carbon of the imidoyl is consistent with our observations for the fluxionality of **5** (Figure 2). The broadened hydride resonance of **8a** sharpens with increasing temperature to +60 °C. In addition, two very minor sharp doublets at −17.49 ($^2J(^{31}P^1H)$ = 15.3 Hz) and −17.89 ($^2J(^{31}P^1H)$ = 15.7 Hz) ppm are observed which remain sharp down to −60 °C. We suggest that these are other rigid conformers of **8b**. The ^{13}C-NMR of a solution of **8a** and **8b** at 25 °C confirms that tripodal rotation at the Ru atom bound to nitrogen is occurring. Two resonances at 205.2 (d, $^2J(^{31}P^{13}C)$ = 9.1 Hz) and

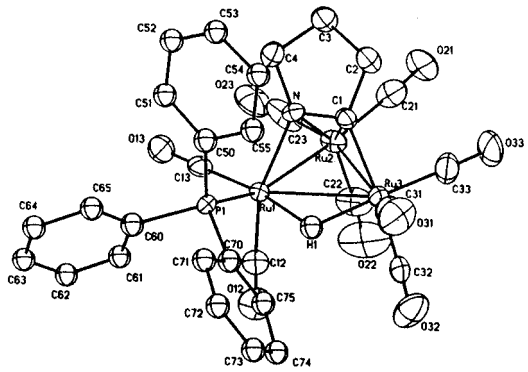

Figure 4. Solid state structure of **9** showing the calculated position of the hydride.

197.3 (d, $^2J(^{31}P^{13}C)$ = 7.6 Hz) ppm appear distinctly broadened at 25 °C. The resonance at 197.2 ppm also shows a hydride coupling in the proton-coupled spectrum. These resonances can then be assigned to the carbonyl groups on the phosphine-substituted ruthenium atom. Significantly, a sharp set of three resonances at 194.62 ($^2J(^{13}C^1H)$ = 14 Hz), 193.72, and 199.55 ppm and a sharp resonance at 197.76 ppm of relative intensity three is observed. A companion set of five resonances of lower intensity which can be assigned to **8b** is also observed. One of the lower intensity set shows a large phosphorous coupling, 204.75 ppm (d, $^2J(^{31}P^{13}C)$ = 7.2 Hz), but is sharp. The specific broadening of the two resonances of the major isomer is consistent with the tripodal motion at the nitrogen bound ruthenium atom and points to the sensitivity of the barrier to these motions toward the groups bound to the imidoyl nitrogen.

In sharp contrast to **2**, the reaction of **3** and **5** with triphenylphosphine yields only one isomer in solution (eqs 4 and 5). A solid state structure of $Ru_3(CO)_8(\mu_3$-

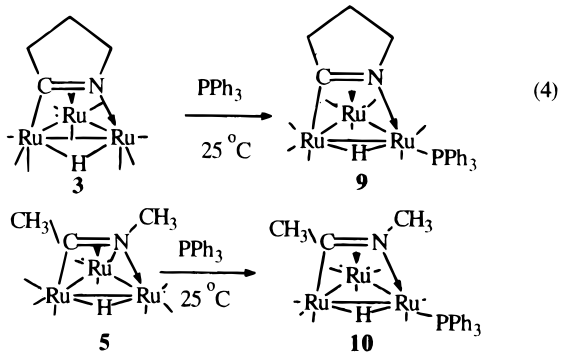

η^2-C=N$(CH_2)_3)(\mu$-H)(PPh_3) (**9**) was obtained to locate the phosphine. The solid state structure of **9** is shown in Figure 4; crystal data are given in Table 1 and selected distances and bond angles in Table 2. The structure consists of an isosceles triangle of ruthenium atoms, with the hydride, whose position was calculated using the program HYDEX,[6] located along the elongated Ru(1)−Ru(3) edge. The pyrrolidine ligand also bridges the Ru(1)−Ru(3) edge, and the phosphine is situated on the Ru atom bound to the nitrogen of the pyrrolidine ligand, exactly as in **8a**. The structure of **9** is identical with the phosphine derivative of the osmium complex, **1**, as deduced from the latter's ^{13}C-NMR.[1i] The ^{13}C-NMR of

(6) Orpen, A. G. *J. Chem. Soc., Dalton Trans.* **1980**, 2509.

Table 1. Crystal Data for 9, 12, and 15

	9	12	15
empirical formula	$C_{30}H_{22}NO_8PRu_3$	$C_{14}H_{12}N_2O_8Ru_3$	$C_{32}H_{25}N_2O_8Os_3P$
fw	858.70	639.47	1167.13
temperature, K	293(2)	293(2)	293(2)
wavelength, Å	0.710 73	0.710 73	0.710 73
cryst syst	monoclinic	monoclinic	monoclinic
space group	$P2_1$ (4)	$P2_1/c$ (14)	$P2_1/c$ (14)
a, Å; α, deg	8.957 (3); 90	11.015(3) 90	9.109(2) 90
b, Å; β, deg	15.952(3); 98.17(2)	10.460(2); 96.73(1)	16.221(3); 90.44(2)
c, Å; δ, deg	11.367(2); 90	17.820(1); 90	22.952(7); 90
volume, Å^3	1608(4)	2039(3)	3391.2(14)
Z	2	4	4
density (calcd), g/cm^3	1.54	2.08	2.307
abs coeff, cm^{-1}	14.3	21.9	113.12
F(000)	810	1224	2172
crystal size, mm^3	0.30 × 0.30 × 0.30	0.40 × 0.35 × 0.30	0.08 × 0.60 × 0.12
θ range for data collection, deg	2.0−26.0	2.0−26.0	1.54−21.98
index ranges	$-10 \le h \le 10$, $0 \le k \le 19$, $-13 \le l \le 13$	$-22 \le h \le 22$, $0 \le k \le 12$, $0 \le l \le 13$	$-9 \le h \le 9$, $0 \le k \le 17$, $-24 \le l \le 24$
abs corr	ψ	ψ	ψ
max and min transmission	1.000 and 0.959	0.999 and 0.812	0.9996 and 0.8829
no. of reflns collected	7184	4448	8658
no. of independent reflns	3277 (R_{int} = 0.029)	4224 (R_{int} = 0.023)	4528 (R_{int} = 0.041)
refinement method	full-matrix least-squares on F^2	full-matrix least-squares on F^2	full-matrix least-squares on F^2
data/restraints/parameters	2172/0/225	3660/0/249	4148/0/410
goodness-of-fit on F^2	0.86	1.77	1.003
final R indices [$I > 2\sigma(I)$]	R1 = 0.0471, wR2 = 0.0421	R1 = 0.0282, wR2 = 0.0316	R1 = 0.0325, wR2 = 0.0585
largest diff peak, e Å^{-3}	0.90(24)	0.37(11)	0.730 and −2.292

Table 2. Selected Distances (Å) and Bond Angles (deg) for 9[a]

	Distances		
Ru(1)−Ru(2)	2.681(1)	N−C(1)	1.32(1)
Ru(1)−Ru(3)	2.973(1)	C1−C2	1.57(2)
Ru(2)−Ru(3)	2.741(2)	C2−C3	1.54(2)
		C3−C4	1.53(2)
Ru(1)−N	2.10(1)		
Ru(3)−C1	2.00(1)		
Ru(2)−N	2.20(1)	Ru−CO[b]	1.88(2)
Ru(2)−C1	2.27(1)	C−O[b]	1.15(2)
Ru(1)−P1	2.358(3)		
	Angles		
Ru(1)−Ru(2)−Ru(3)	66.50(4)	C(50)−P(1)−C(60)	106.6(1)
Ru(2)−Ru(1)−Ru(3)	57.72(4)	C(50)−P(1)−C(70)	103.4(1)
Ru(1)−Ru(3)−Ru(2)	55.78(3)	C(60)−P(1)−C(70)	99.8(1)
Ru(2)−Ru(1)−P(1)	153.36(9)	C(1)−N−C(4)	113(1)
Ru(1)−Ru(2)−C(1)	69.3(3)	N−C(1)−C(2)	109(1)
Ru(2)−Ru(3)−C(1)	54.5(4)	N−C(4)−C(3)	104.7(9)
Ru(1)−Ru(2)−N	49.8(2)	C(1)−C(2)−C(3)	103(1)
Ru(3)−Ru(2)−N	70.0(2)	C(2)−C(3)−C(4)	104(1)
Ru−C−O[b]	176(2)		

[a] Numbers in parentheses are estimated standard deviations. [b] Average values.

9 in the carbonyl region is also identical to its osmium analog showing six resonances in a ratio of 1:1:3:1:1:1 at 200.47 (d, $^2J(^{31}P^{13}C)$ = 2.2 Hz), 198.55, 196.83, 195.95, (d, $^2J(^{31}P^{13}C)$ = 5.5 Hz), 194.20, and 191.67 ppm, respectively. These data (X-ray and NMR) reveal virtually identical structural and dynamical properties for **9** and its osmium analog. No change in the appearance of the hydride resonance is observed down to −60 °C. Thus, other conformers of **9** are not appreciably populated as for **8a** and **8b**.

The structure of $Ru_3(CO)_8(\mu_3$-η^2-$CH_3C{=}NCH_3)(\mu$-H)-PPh_3 (**10**) is the same as **9** based on its ^{1}H- and ^{13}C-NMR data. The ^{13}C-NMR of **10** remains unchanged down to −80 °C. The assignments made based on the ^{31}P−^{13}C and ^{1}H−^{13}C coupling constants are verified by a ^{13}C−^{13}C-COSY experiment performed on a sample of **10** >90% enriched with ^{13}CO (Figure 5). In addition to confirming our assignments based on the 1D data, note the cross peak observed between carbonyls a and d

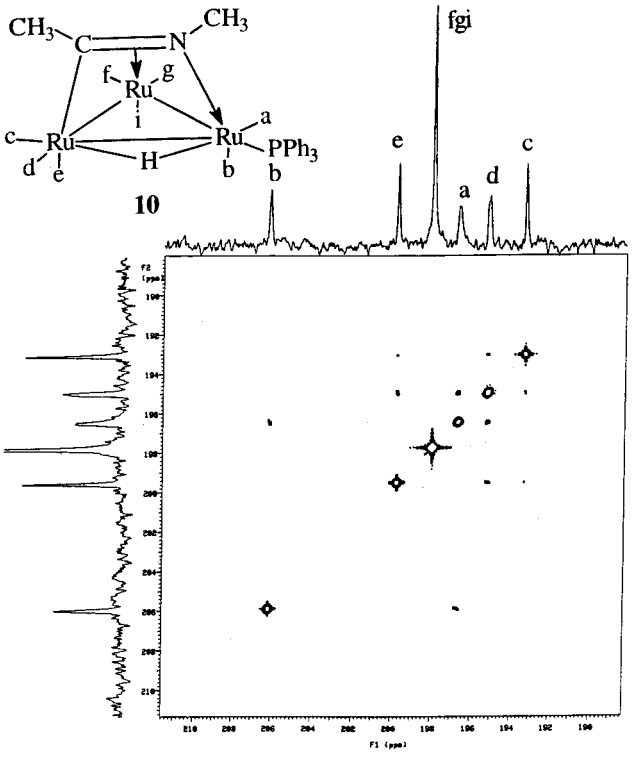

Figure 5. 2D-^{13}C−^{13}C-COSY spectrum of **10** at 25 °C in $CDCl_3$ at 100 MHz.

which establish their *trans* relationship and suggest that such three-bond couplings should be useful for carbonyl assignments in other clusters. The 2D-^{13}C-EXY spectrum of this sample showed no cross peaks at 25 °C. From the above data it cannot be determined whether the windshield wiper motion has been stopped by phosphine substitution in **8**−**10** because the asymmetry in these clusters makes it a hidden process. Phosphine substitution does slow down tripodal motion at the Ru atom bound to nitrogen relative to the Ru atom bound to the C−N double bond, while the carbonyls on the Ru atom bound to carbon remains rigid on

the NMR time scale as in **2**−**5**. The observed greater rigidity at the nitrogen bound Ru atom does imply that the windshield wiper motion is slow on the NMR time scale in **8**−**10**. The lower barrier to tripodal motion at the nitrogen bound Ru atom in **8b** relative to **9** and **10** reflects the steric crowding introduced by the bulkier ethyl group in **8b** relative to the ring methylene in **9** and the methyl group in **10**.

In order to understand the stepwise pathway for the formation of **8**−**10** and related compounds, we conducted a series of NMR experiments where equimolar amounts of **5** and PPh_3 were combined in an NMR tube at room temperature and the reactions monitored by ^{1}H-NMR for about 72 h. Upon addition of the phosphine, an instant color change from yellow to orange occurred. The ^{1}H-NMR revealed that all of **5** had been consumed and three new resonances appeared in the hydride region at −14.24 ($^2J(^{31}P^1H)$ = 10.8 Hz), −14.71 (singlet) attributable to **6** and −17.4 ($^2J(^{31}PH)$ = 14.4 Hz) ppm attributable to **10**. The ratio of these peaks was initially observed to be 9:2:1, and the peaks attributable to **6** and **10** gradually increased with time. The resonance at −14.24 ppm must belong to a species where the phosphorus is on a ruthenium atom bridged by the hydride ligand given the size of the phosphorus−hydrogen two-bond coupling. Furthermore, the chemical shift of this resonance is similar to that of other decacarbonyl hydrides in the μ-η^2-imidoyl family.[1] Significantly, no $^3J(^{31}P^1H)$ coupling to the methyl groups of the imidoyl ligand is observed as for **8b** and **10** ($^2J(^{31}P^1H)$ = 3.0 Hz for both). These data suggest a general structural type for this phosphine addition product, $Ru_3(CO)_9(\mu$-η^2-$CH_3C{=}NCH_3)(\mu$-H)PPh_3 (**11a**), similar to structures **B** and **C** (Scheme 2). In order to confirm the structure of this intermediate, we examined the ^{13}C-NMR of a ^{13}CO-enriched sample of **5** which was treated with 1.2 equiv of triphenylphosphine. This solution shows two complex multiplets at 210.9 and 209.9 ppm which are identical in pattern to the multiplets obtained when solutions of **5** are treated with carbon monoxide to give **6**. The chemical shift of the most downfield resonances of **6** are 209.2 and 207.3 ppm, which are very similar to those observed for this intermediate, **11a**. No hydride or phosphorus couplings are observed in **11a**. Furthermore, when **10** is treated with carbon monoxide, the observed ^{1}H- and ^{13}C-NMR are identical to those of **11a**. Taken together, these experiments point to a species which contains an $Ru(CO)_4$ moiety for **11a** with the complex multiplet arising from ^{13}C−^{13}C couplings from the mixture of isotopomers at the $Ru(CO)_4$ group. Attempts to isolate this intermediate were unsuccessful since, on chromatography, **11a** converts to **10**. This evidence confirms a structure for **11a** where the hydride and the imidoyl bridge a common edge of the Ru_3 triangle and phosphine is located on the Ru atom bound to either the carbon or the nitrogen of the imidoyl ligand (Scheme 2, structures **B** and **C**).

A similar set of experiments was conducted with **2** and triphenylphosphine. Overall, the results were very similar except for one significant difference. After the initial addition of triphenylphosphine, two partially overlapping doublets at −14.23 ($^2J(^{31}P^1H)$ = 12.2 Hz) and −14.25 ($^2J(^{31}P^1H)$ = 12.0 Hz) instead of one are observed. On standing in solution, gradual conversions to **8a** and **8b** are observed at approximately the same rate. As for **5**, these same two doublets are observed when solutions containing **8a** and **8b** are treated with carbon monoxide. As for **11a**, the ^{13}C-NMR of these two intermediates (Scheme 2, **B** and **C**) shows two complex multiplets with no apparent ^{31}P or ^{1}H coupling. Thus, the presence of an ethyl group instead of a methyl group on the nitrogen results in the formation of two intermediate adducts which convert directly to **8a** and **8b**. In order for this transformation to occur at the same rate for both **8a** and **8b** without ligand dissociation/association (which is slower than the rate of conversion), migration by both nitrogen and carbon is required (Scheme 2) to form **8a** and **8b**, respectively.

These results and those obtained for the addition of CO to **2**−**5** represent the first definitive evidence supporting carbon migration in μ_3-η^2-imidoyls.[1m] That the osmium analogs do not exhibit this behavior except at much more elevated temperatures is understandable in light of the expected greater strength of osmium−carbon bonds.

C. Reactions of 2 and 3 with Methyl Isocyanide. The reactions of **2** and **3** with methyl isocyanides do not proceed as cleanly as with triphenylphosphine. The further reaction of the methyl isocyanide ligand with the μ-hydride to give μ-methylbisimidoyl derivatives of **2** and associated nonspecific decomposition seem to be the chief causes of the difficulty in obtaining good yields of $Ru_3(CO)_8(\mu_3$-η^2-$CH_3C{=}NCH_2CH_3)(\mu$-H)$(CNCH_3)$ (**12**) and $Ru_3(CO)_8(\mu_3$-η^2-$C{=}N(CH_2)_3(\mu$-H)$(CNCH_3)$ (**13**) eqs 6 and 7). This is evidenced by the appearance of a

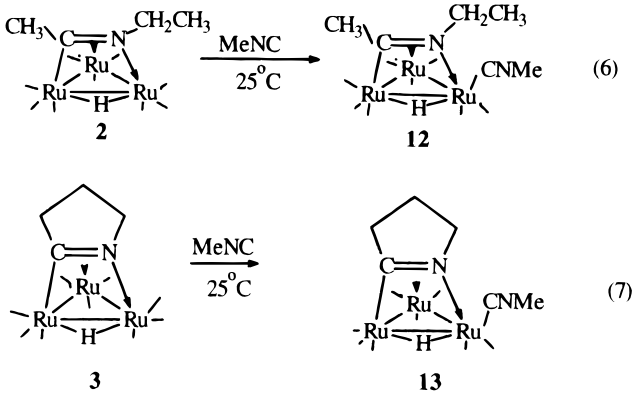

resonance at 9.8 ppm when solutions of **12** are allowed to stand in deuteriochloroform. These relatively labile ruthenium complexes may also catalyze polymerization of methyl isocyanide. These factors made accurate elemental analysis difficult to obtain. Furthermore, the infrared spectra were uncharacteristically ill-defined due to the presence of many isomers in solution (*vide infra*). We were, however, able to obtain a solid state structure of **12** by X-ray diffraction methods. The solid state structure of **12** is shown in Figure 6, crystal data are given in Table 1, and selected distances and angles are given in Table 3. The structure of **12** consists of an isosceles triangle of Ru atoms with the hydride ligand located along the same elongated Ru(2)−Ru(3) edge as the μ_3-imidoyl ligand. The isocyanide ligand is situated on the Ru atom bound to the nitrogen of the imidoyl ligand and *trans* to the hydride ligand. This overall structure is identical to the osmium analog of **12**.[5] The bond lengths and angles of the imidoyl ligand are very similar to those in **8a** and **9**. The ^{1}H-NMR spectra of

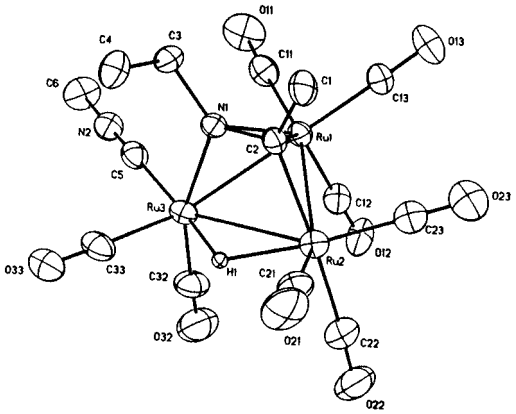

Figure 6. Solid state structure of **12** showing the calculated position of the hydride.

Table 3. Selected Distances (Å) and Bond Angles (deg) for 12[a]

	Distances		
Ru(1)−Ru(2)	2.737(1)	N(1)−C(2)	1.35(1)
Ru(1)−Ru(3)	2.685(1)	N(1)−C(4)	1.49(1)
Ru(2)−Ru(3)	2.904(1)	N(2)−C(6)	1.15(1)
Ru(1)−C(2)	2.21(1)	N(2)−C(7)	1.45(1)
Ru(1)−C(2)	2.25(1)	C(1)−C(2)	1.54(1)
Ru(2)−C(2)	2.06(1)	C(4)−C(5)	1.53(1)
Ru(3)−N(1)	2.10(1)	C−O[b]	1.13(1)
Ru(3)−C(6)	1.98(1)		
Ru−CO[b]	1.90(1)		
	Angles		
Ru(1)−Ru(2)−Ru(3)	56.74(1)	C(2)−N(1)−C(4)	122.6(4)
Ru(1)−Ru(3)−Ru(2)	58.49(1)	N(1)−C(2)−C(1)	120.6(4)
Ru(2)−Ru(1)−Ru(3)	64.76(1)	N(1)−C(4)−C(5)	110.4(4)
Ru(3)−C(5)−N(2)	174.9(5)	C(6)−N(2)−C(7)	174.7(5)
Ru(1)−Ru(3)−N(1)	53.2(1)		
Ru(2)−Ru(3)−N(1)	67.8(1)		
Ru(1)−Ru(2)−C(2)	53.6(1)		
Ru(3)−Ru(2)−C(2)	68.3(1)		
Ru−C−O[b]	172.7(6)		

[a] Numbers in parentheses are estimated standard deviations. [b] Average values.

12 and **13** show broadened hydride resonances at −18.48 and −19.02 ppm, respectively. As the temperature is lowered to −72 °C, six sharp hydride resonances are resolved at −17.83, −17.98, −18.17, −19.05, −19.35, −19.43 ppm (rel int = 1.0:2.5:5.0:2.0:22.0:0.8) and −17.78, −18.13, −18.28, −19.15, −19.50, −19.63 ppm (rel int = 1.0:1.6:2.0:1.2:8.4:0.8) for **12** and **13**, respectively. The virtually identical hydride region spectra obtained for **12** and **13** illustrate that, for the less bulky isocyanide ligand, the presence of the ethyl group in **10** has little impact on the isomer distribution as was the case for **8** *versus* **9** and **10**. The existence of exactly six isomers for **12** and **13** can be explained by the population of all the positional isomers which can be interchanged by a combination of axial−radial exchange and the windshield wiper motion.[5] The analogous osmium compounds exhibit the same behavior.[5] Attempts to follow this reaction by ^{1}H-NMR were thwarted by the large number of isomers produced during the addition step and decomposition. The osmium analog of **13** exhibits the same distribution of isomers, but since it is obtained from its nonacarbonyl precursor at 125 °C, additional isomers are observed which are formed by dissociation/association pathways.[5]

D. Sequential Additions of Phosphines and Isocyanides to 1. In the introduction to this report, we suggested that the hemilabile nature of the imidoyl ligand should enable sequential addition of ligands according to Scheme 2 (i.e., μ_3 to μ to μ_3 to μ-imidoyl conversions). In the case of the ruthenium systems such as **8** and **10**, stepwise ligand addition has been attempted, but leads to extensive cluster fragmentation. However, in the case of **1**, this type of sequential addition of two different ligands has been successfully demonstrated. Thus, reaction of PPh_3 with **1** followed by thermolysis according to Scheme 2 yields $Os_3(CO)_8$-(μ_3-η^2-C=N$(CH_2)_3$)PPh_3 (**14**) as previously reported.[1i] Treatment of **14** with methyl isocyanide at room temperature leads to the formation of $Os_3(O)_8$(μ-η^2-C=N-$(CH_2)_3$)(μ-H)$PPh_3(CH_3NC)$ (**15**) in good yield (eq 8). The

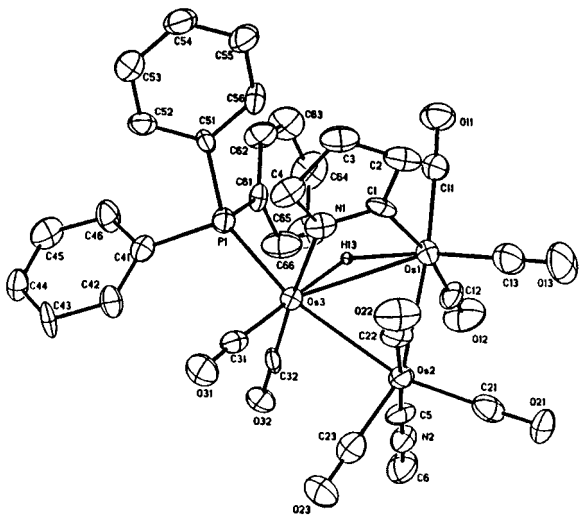

Figure 7. Solid state structure of **15** showing the calculated position of the hydride.

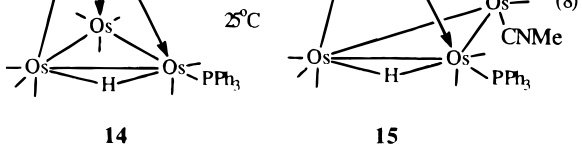

14 **15** (8)

fact that the overall rate of addition of methyl isocyanide to **14** is similar to that of **1** (complete reaction in ∼24 h at 25 °C) demonstrates that phosphine substitution at the imidoyl edge of the cluster has no significant influence on the rate of displacement of the carbon−nitrogen double bond. In order to understand whether the geometry of the isocyanide adduct would be influenced by the presence of the bulky triphenylphosphine group, we undertook a solid state structural investigation of **15** which is shown in Figure 7, crystal data are given in Table 1, and selected distances and bond angles are given in Table 4. The overall geometry of **15** is similar to that of other μ-η^2-triosmium imidoyl clusters previously reported.[5]

Interestingly, however, the methyl isocyanide ligand in **15** is in the axial position on the opposite face of the Os_3 triangle as the imidoyl ligand, whereas in $Os_3(CO)_9$(μ-η^2-C=N$(CH_2)_3$)(μ-H)(CH_3NC) it is on the same face of the cluster. This same *anti* arrangement of the imidoyl and the isocyanide ligands is found in $Os_3(CO)_9$(μ-η^2-C=N$(CH_2)_3$)(μ-H)$((CH_3)_3CNC)$.[5] This is most likely a consequence of the presence of the phosphine ligand

Table 4. Selected Distances (Å) and Bond Angles (deg) for 15[a]

	Distances		
Os(1)−Os(2)	2.8538(7)	N(1)−C(1)	1.284(6)
Os(1)−Os(3)	2.9483(7)	C(1)−C(2)	1.459(6)
Os(2)−Os(3)	2.8490(8)	C(2)−C(3)	1.496(6)
Os(1)−C(1)	2.103(4)	C(3)−C(4)	1.520(2)
Os(3)−N(1)	2.103(3)	C(4)−N(1)	1.512(6)
Os(3)−P(1)	2.373(1)	C(5)−N(2)	1.131(6)
Os(2)−C(5)	1.995(4)	C(6)−N(2)	1.420(6)
Os−CO[b]	1.881(5)	P(1)−C[b]	1.823(4)
		C−O[b]	1.145(6)
	Angles		
Os(1)−Os(2)−Os(3)	62.26(2)	N(1)−C(1)−C(2)	112.2(4)
Os(1)−Os(3)−Os(2)	58.95(2)	C(1)−N(1)−C(4)	111.4(4)
Os(2)−Os(1)−Os(3)	58.79(2)	C(5)−N(2)−C(6)	174.7(4)
Os(2)−Os(1)−C(1)	86.88(1)	C(41)−P(1)−C(51)	103.2(2)
Os(2)−Os(3)−N(1)	88.20(1)	C(41)−P(1)−C(61)	100.4(2)
Os(2)−C(5)−N(2)	173.2(4)	C(51)−P(1)−C(61)	104.0(2)
Os(2)−Os(3)−P(1)	163.67(3)		
Os−C−O[b]	176.5(5)		

[a] Numbers in parentheses are estimated standard deviations. [b] Average values.

which forces the plane of the imidoyl ligand to adopt a slightly acute angle with the Os_3 plane (~87.5°). In $Os_3(CO)_{10}(\mu\text{-}\eta^2\text{-}C{=}N(CH_2)_3)(\mu\text{-}H)$, this angle is essentially 90°.[5,7] However, the factors controlling which face of the cluster a ligand on the unbridged osmium atom occupies are quite subtle. There may be other structural features such as the disposition of the carbonyls which control this stereochemistry. A common theme which runs through all of the chemistry reported here are the substantive changes in product structure which result from relatively minor changes in reactant stereochemistry.

Experimental Section

All reactions were carried out under a nitrogen atmosphere using standard inert atmosphere techniques. Reactions were worked up in the air using thin layer chromatography (20 × 40 × 0.1 cm silica gel PF-254, EM) or column chromatography (60−200 mesh silica gel, Aldrich). Methylene chloride was distilled from calcium hydride, benzene from sodium benzophenone ketyl, and hexane was dried over sodium and stored over molecular sieves (4A Mallincrodt). Triphenylphoshine, methyldiethylamine, and (methoxymethyl)pyrrolidine were purchased from Aldrich and used as received. Methyl isocyanide was synthesized by literature procedures.[8] Compounds **1**−**4** and **14** were prepared by published literature procedures.[1c,f,i] NMR spectra were measured on a Varian Unity Plus 400 or a JEOL EX 400 NMR spectrometer. Infrared spectra were obtained on a Perkin-Elmer 1600 FT-IR. Elemental analyses were performed by Schwarzkoff Microanalytical Labs, Woodside, NY.

Synthesis of $Ru_3(CO)_9(\mu_3\text{-}\eta^2\text{-}CH_3C{=}NCH_3)(\mu\text{-}H)$ (5). $Ru_3(CO)_{12}$ (380 mg, 0.59 mmol), 360 μL (3.9 mmol) of freshly distilled $CH_3(CH_3CH_2)_2N$, and 99 mg (1.31 mmol) of $(CH_3)_3NO$ were combined with 150 mL of benzene and refluxed for 8 h. The reaction mixture was cooled, filtered, and rotary evaporated, and the residue was taken up in minimum methylene chloride and chromatographed using hexanes as eluent. Three yellow-orange bands were eluted. The fastest moving band contained 21 mg (5.5%) of $Ru_3(CO)_{10}(\mu_3\text{-}\eta^2\text{-}CH_3C{=}NCH_3)(\mu\text{-}H)$ (**6**); the second band contained 67 mg (18%) of $Ru_3(CO)_9(\mu_3\text{-}\eta^2\text{-}CH_3C{=}NCH_2CH_3)(\mu\text{-}H)$ (**2**); the third band contained 91 mg (26%) of $Ru_3(CO)_9(\mu_3\text{-}\eta^2\text{-}CH_3C{=}NCH_3)(\mu\text{-}H)$ (**5**).

Spectroscopic and Analytical Data for 5. Anal. Calcd for $C_{12}H_7O_9NRu_3$: C, 23.53; H, 1.14; N, 2.28. Found: C, 22.96; H, 1.25; N, 2.34. IR (ν(CO), hexane): 2071 (m), 2062 (w), 2038 (vs), 2022 (m), 1992 (m, br), 1966 (w, br) cm^{-1}. ^{1}H-NMR ($CDCl_3$): 3.52 (s, 3H), 2.67 (s, 3H), −18.14 (s, 1H) ppm. ^{13}C-NMR (CD_2Cl_2, −90 °C, carbonyl region): 205.15 (1C), 199.41 (1C), 198.14 (1C), 193.11 (1C, $2J(^1H^{13}C)$ = 10.7 Hz), 191.44 (3C), 191.11 (1C), 185.86 (1C) ppm.

Spectroscopic and Analytical Data for 6. Anal. Calcd for $C_{13}H_7O_{10}NRu_3$: C, 24.38; H, 1.10; N, 2.19. Found: C, 25.12; H, 1.16; N, 1.85. IR (ν(CO), hexane): 2099 (w), 2062 (vs), 2048 (s), 2021 (s), 2013 (s), 1996 (m, br), 1979 (w, br) cm^{-1}. ^{1}H-NMR ($CDCl_3$): 3.23 (s, 3H), 2.32 (s, 3H), −14.71 (s, 1H) ppm. ^{13}C-NMR ($CDCl_3$, carbonyl region) 209.20 (m, 1C), 207.33 (m, 1C), 201.90 (s, 2C), 196.75 (s, 1C), 195.80 (s, 1C), 192.25 (s, 1C), 191.9 (s, 1C), 190.60 (s, 1C), 186.95 (s, 1C) ppm.

Synthesis of the Triphenylphosphine Derivatives 8−10. Thirty milligrams (0.05 mmol) of **2**, **3**, or **5** was dissolved in 25 mL of hexane, and 1.2 equiv (16 mg) of triphenylphosphine was added to the yellow solution. As the triphenylphosphine dissolved, the solution turned immediately orange, and this solution was stirred for an additional 30 min. The reaction solution was rotary evaporated, taken up in methylene chloride, and chromatographed with methylene chloride−hexanes (1:4) to yield a fast-moving yellow mirror band and a major yellow/orange band containing 30−35 mg (70−82%) of **8**, **9**, or **10**.

Spectroscopic and Analytical Data for 8. Anal. Calcd for $C_{30}H_{24}NO_8PRu_3$: C, 41.82; H, 2.79; N, 1.63. Found: C, 41.25; H, 3.02; N, 1.78. IR (ν(CO), cyclohexane): 2068 (m), 2056 (m), 2030 (vs), 2009 (vs), 1986 (s, br), 1971 (w), 1868 (m, br). ^{1}H-NMR **8a** ($CDCl_3$): 7.45 (m, 15H), 3.00 (m, 1H), 2.71 (s, 3H), 2.51 (m, 1H), 0.77 (t, 3H), −17.20 (d, 1H, $^2J(^{31}PH)$ = 15.2 Hz) ppm. **8b**: 7.45 (m, 15H), 3.99 (m, 1H), 3.09 (m, 1H), 2.21 (d, 3H, $^4J(^{31}P^1H)$ = 2.9 Hz), 1.12 (t, 3H), −17.47 ($^2J(^{31}P^1H)$ = 15.3 Hz) ppm. ^{13}C-NMR **8a** (CD_2Cl_2, carbonyl region): 205.17 (d, br, 1C, $^2J(^{31}P^{13}C)$ = 9.1 Hz), 199.55 (s, 1C), 197.76 (s, 3C), 197.28 (d, br, 1C, $^2J(^{31}P^{13}C)$ = 7.6 Hz), 194.6 (s, 1C), 193.72 (s, 1C) ppm. **8b**: 204.75 (d, $^2J(^{31}P^1H)$ = 7.2 Hz, 1C), 194.75 (s, 1C), 197.95 (s, 3C), 196.45 (d, 1C, $^2J(^{31}P^{13}C)$ = 4.6 Hz), 194.98 (s, 1C), 193.06 (s, 1C).

Spectroscopic and Analytical Data for 9. Anal. Calcd for $C_{30}H_{22}O_8NPRu_3$: C, 41.91; H, 2.58; N, 1.63. Found: C, 42.36; H, 2.99; N, 1.87. IR (ν(CO), hexane): 2060.8 (m), 2031 (vs), 2011 (s), 1984 (br, w), 1971 (br, w) cm^{-1}. ^{1}H-NMR (CD_2Cl_2): 7.42 (m, 15H), 3.09 (dd, 1H), 2.93 (dd, 1H), 2.54 (m, 1H), 1.98 (m, 1H), 1.77 (m, 1H), 1.36 (m, 1H), −17.53 (d, 1H, $^2J(^{31}P^1H)$ = 13.4 Hz) ppm. ^{13}C NMR ($CDCl_3$, carbonyl region): 200.47 (d, 1C, $^2J(^{31}P^{13}C)$ = 2.2 Hz), 198.55 (s, 1C), 196.83 (s, 3C), 196.95 (d, 1C, $^2J(^{31}P^{13}C)$ = 5.5 Hz), 194.20 (s, 1C), 191.67 (s, 1C).

Analytical and Spectroscopic Data for 10. Anal. Calcd for $C_{29}H_{22}NO_8PRu_3$: 41.13; H, 2.62; N, 1.65. Found: C, 41.23; H, 2.54; N, 1.52. IR (ν(CO), hexane): 2070 (m), 2048 (w), 2032 (vs), 2010 (vs), 1985 (m, br), 1974 (w). ^{1}H-NMR ($CDCl_3$): 7.41 (m, 15H), 2.83 (s, 3H), 2.55 (d, 3H, $^4J(^{31}PH)$ = 1.8 Hz), −17.40 (d, 1H, $^2J(^{31}P^1H)$ = 14.4 Hz). ^{13}C-NMR ($CDCl_3$, carbonyl region): 205.16 (d, 1C, $^2J(^{31}P^{13}C)$ = 2.2 Hz), 198.75 (s, 1C), 197.10 (s, 3C), 196.04 (d, 1C, $^2J(^{31}P^{13}C)$ = 5.5 Hz), 194.42 (s, 1C), 192.6 (s, 1C) ppm.

Synthesis of the Methyl Isocyanide Derivatives for 12 and 13 from 2 and 3. **2** and **3** (25−30 mg, 0.05 mmol) were combined with 50 mL of hexane and 2 μL (~1 equiv) of MeNC in a Schlenk tube and stirred for 4 h. The cloudy orange solution was rotary evaporated and chromatographed with methylene chloride−hexane (1:4) to yield two yellow bands. The faster moving band was unreacted starting material, and the slower moving band contained **12** or **13** (10−15 mg, 32−46%).

Spectroscopic Data for 12. ^{1}H-NMR (CD_2Cl_2, −72 °C) major isomer (68%): 3.85 (m, 1H), 3.51 (s, 3H), 3.06 (m, 1H), 2.67 (s, 3H), 1.15 (t, 3H), −19.35 (s, 1H) ppm.

(7) Kabir, S. E.; Rosenberg, E.; Day, M.; Hardcastle, K. I.; Wolf, E.; McPhillips, T. *Organometallics* **1995**, *14*, 721.

(8) Shuster, R. E.; Scott, J. E.; Casanova, J. *Organic Syntheses*; Wiley: New York, 1973; Collect. Vol. 5, p 772.

Spectroscopic Data for 13. ^{1}H-NMR (CD_2Cl_2, −72 °C) major isomer (55%): 3.51 (s, 3H), 3.15 (m, 1H), 2.66 (m, 1H), 2.40 (m, 1H, br), 1.49 (m, 1H), 1.35 (m, 1H), 0.77 (m, 1H), −19.35 (s, 1H) ppm.

Synthesis of $Os_3(CO)_8(\mu$-η^2-C=N$(CH_2)_3)(\mu$-H)P$(C_6H_5)_3$-(CH_3NC). $Os_3(CO)_8(\mu$-η^2-C=N$(CH_2)_3)(\mu$-H)$(P(C_6H_5)_3$ (30 mg, 0.027 mmol) was dissolved in 30 mL of hexane in a 100 mL Schlenk tube and cooled to −10 °C. A 5-fold excess of methyl isocyanide (15 μL) was syringed in and stirred for 24 h. The clear yellow solution was chromatographed using methylene chloride−hexane (1:4). Two bands were eluted; the faster moving band was identified as **15**, 23 mg (78%).

Spectroscopic and Analytical Data for 15. Anal. Calcd for $C_{32}H_{25}N_2O_8Os_3P$: C, 32.93; H, 2.16; N, 2.40. Found: C, 33.16; H, 2.48; N, 2.76. IR (ν(CO), chloroform) 2050 (m), 2019 (vs), 1989 (s), 1969 (m, br), 1959 (w, br), 1936 (w, br). ^{1}H-NMR ($CDCl_3$): 7.39 (m, 15H), 3.64 (s, 3H), 3.09 (m, 2H), 3.41 (m, 2H), 2.23 (m, 2H), −14.11 (d, $^2J(^{31}P^{13}C) = 10.4$ Hz) ppm.

NMR-Monitored Reactions with Carbon Monoxide or Triphenylphosphine. Samples (20−25 mg) of **2**−**5** were dissolved in 0.6 mL of $CDCl_3$ or CD_2Cl_2 in a 5 mm NMR tube. The solutions were degassed by three freeze−thaw cycles and then frozen and filled to ∼1 atm with carbon monoxide. The samples were allowed to come to room temperature, shaken, and then monitored by ^{1}H- and/or ^{13}C-NMR. A similar procedure was used for triphenylphosphine except that the samples were dissolved in 0.4 mL of solvent and 0.2 mL of a solution containing 1.0−1.2 equiv of triphenylphosphine was added by syringe.

X-ray Structure Determination of 9, 12, and 15. Crystals of **9**, **12**, and **15** for X-ray examination were obtained from saturated solutions of each in hexane/dichloromethane solvent systems at −20 °C. Suitable crystals of each were mounted on glass fibers, placed in a goniometer head on the Enraf-Nonius CAD4 diffractometer, and centered optically. Unit cell parameters and an orientation matrix for data collection were obtained by using the centering program in the CAD4 system. Details of the crystal data are given in Table 1. For each crystal, the actual scan range was calculated by scan width = scan range + 0.35 tan θ, and backgrounds were measured by using the moving-crystal moving-counter technique at the beginning and end of each scan. Two representative reflections were monitored every 2 h as a check on instrument and crystal stability, and an additional two reflections were monitored periodically for crystal orientation control. Lorentz, polarization, and decay corrections were applied, as was an empirical absorption correction based on a series of ψ scans for each crystal. The weighting scheme used during refinement for all structures was $1/\sigma^2$.

Each of the structures was solved by the Patterson method using SHELXS-86,[9] which revealed the positions of the metal atoms. All other non-hydrogen atoms were found by successive difference Fourier syntheses. The expected hydride positions for each compound were calculated by using the program HYDEX,[6] but other hydrogen atoms were included only for structure **15** and were placed in their expected chemical positions using the HFIX command in SHELXL-93.[10] The hydrides were given fixed positions and *U*'s, and the other hydrogen atoms in **15** were included as riding atoms in the final least squares refinements with *U*'s which were related to the atoms ridden upon. All other non-hydrogen atoms were refined anisotropically.

Scattering factors were taken from Cromer and Waber.[11] Anomalous dispersion corrections were those of Cromer.[12] All other data processing for **9** and **12** was carried out on a DEC Micro VAX II using the MolEN programs, and for **15**, on a DEC 3000 AXP computer using the Open MolEN system of programs.[13] Structure refinement and preparation of figures and tables for publication were carried out on PC's using SHELXL-93[10] and XP/PC-13 programs.[14]

Acknowledgment. We gratefully acknowledge the National Science Foundation (E.R., CHE9394615 and CHE9624367), the Consiglio Nazionale delle Ricerche (L.M.), the Ministry of University and Scientific Research (L.M.), and the University of Turin (E.R.) for support of this research.

Supporting Information Available: Tables 5−13 listing complete bond distances and angles, atomic coordinates, and anisotropic displacement parameters for **9**, **12**, and **15** (22 pages). Ordering information is given on any current masthead page.

OM961090C

(9) Sheldrick, G. M. *Acta Crystallogr.* **1990**, *A46*, 467.
(10) Sheldrick, G. M. *Program for Structure Refinement*; University of Goettingen: Goettingen, Germany, 1993.
(11) Cromer, D. T.; Waber, J. T. *International Tables for X-ray Crystallography*; Kynoch: Birmingham; 1974; Vol. 4, Table 2.2B.
(12) Cromer, D. T. *International Tables for X-ray Crystallography*; Kynoch: Birmingham, 1974; Vol. 4, Table 2.3.1.
(13) Fair, C. Kay. "*MolEN*" *Structure Determination System*; Enraf-Nonius: Delft, The Netherlands, 1990.
(14) "XP/PC" *Molecular Graphics Software*; Siemans Analytical X-ray Instruments, Inc.: Madison, WI.